Stereoselective Diamine Chelates of a Chiral Lithium Amide Dimer: New Insights into the Coordination Chemistry of Chiral Lithium Amides

Per I. Arvidsson, Göran Hilmersson,* and Per Ahlberg

Contribution from the Department of Chemistry, Organic Chemistry, Göteborg University, SE-412 96 Göteborg, Sweden

Received August 3, 1998

Abstract: The chiral lithium amide (*S*)-2-(1-pyrrolidinylmethyl)pyrrolidide, Li-**1**, which is extensively used in stereoselective synthesis, yields (Li-**1**)$_2$/**1** chelates in the presence of the corresponding diamine **1** as shown by dynamic NMR spectroscopy. The lithium amide Li-**1** has low solubility in DEE, but the chelate (Li-**1**)$_2$/**1** is highly soluble. The diamine TMEDA also forms a chelate with dimeric Li-**1**, (Li-**1**)$_2$/TMEDA. Uncomplexed diamine **1** exhibits ligand exchange with complexed **1** in (Li-**1**)$_2$/**1** by a dissociative mechanism ($\Delta G^{\ddagger}_{175K} = 7.8$ kcal mol^{-1}). The (Li-**1**)$_2$/**1** chelate undergoes a fast intra-complex diamine−amide interconversion via degenerate proton transfer between diamine and amide ($\Delta G^{\ddagger}_{268K} = 10.9$ kcal mol^{-1}). Computational studies, using semi-empirical (PM3) and density functional (B3LYP) methods, show the stabilities of the complexes in agreement with experiments.

Introduction

Organolithium compounds are, due to their versatility and generality, among the most important reagents in organic synthesis. They react both as nucleophiles, e.g. carbon−carbon bond formation, and as bases. Despite tremendous interest in asymmetric synthesis over the past decades, only a few asymmetric applications using organolithium compounds have been reported. Chiral lithium amides are, due to their high basicity and low nucleophilicity, excellent reagents for preparation of enantiopure compounds.[1,2] These reagents are used primarily as enantioselective deprotonation reagents, but have also been used in other lithiation reactions.[3−5] Despite the importance of chiral lithium amides for asymmetric synthesis, knowledge about the structure and dynamics of this important class of compounds is still meagre. Further insight into the structure of these reagents will form the basis for a deeper understanding of their reactivity.

Organolithium reagents are often misleadingly treated as simple monomers, although it is well-known that they form aggregates, rapidly equilibrating.[6] Studies by Collum and coworkers have shown that the reactivity of these aggregates is highly dependent on aggregate size and solvation.[7−10] They also demonstrated that secondary amines are excellent solvents for lithium amides.[11] This finding is of particular importance since amines are generated when lithium amides are used in deprotonation reactions.[12]

Most chiral lithium amides used in enantioselective deprotonation reactions contain internal coordinating groups (often pyrrolidine or methoxy) separated from the amide nitrogens by two carbons, giving five-membered rings upon complexation.[13−15]

For example, lithium salts of proline derived ligands, such as (*S*)-2-(1-pyrrolidinylmethyl)pyrrolidine **1**, i.e., Li-**1**, have been used extensively for enantioselective deprotonation of achiral epoxides.[16−20] The ring opening of cyclohexene oxide **2** by Li-**1**

(1) Cox, P. J.; Simpkins, N. S. *Tetrahedron: Asymmetry* **1991**, *2*, 1−26.
(2) Koga, K. *Pure Appl. Chem.* **1994**, *66*, 1487−1492.
(3) Hodgson, D. M.; Gibbs, A. R.; Lee, G. P. *Tetrahedron* **1996**, *52*, 14361−14384.
(4) Bhuniya, D.; DattaGupta, A.; Singh, V. K. *J. Org. Chem.* **1996**, *61*, 6108−6113.
(5) O'Brien, P. *J. Chem. Soc., Perkin Trans. 1* **1998**, 1439−1457.
(6) (a) Fraenkel, G.; Henrichs, M.; Hewitt, J. M.; Su, B. M.; Geckle, M. J. *J. Am. Chem. Soc.* **1980**, *102*, 3345. (b) Seebach, D.; Hässig, R.; Gabriel, J. *Helv. Chim. Acta* **1983**, *66*, 308. (c) Bauer, W.; Winchester, W. R.; Schleyer, P. v. R. *Organometallics* **1987**, *6*, 2371. (d) Gregory, K.; Schleyer, P. v. R.; Snaith, R. *Adv. Inorg. Chem.* **1991**, *37*, 47. (e) Collum, D. B. *Acc. Chem. Res.* **1993**, *26*, 227−234.
(7) Lucht, B. L.; Bernstein, M. P.; Remenar, J. F.; Collum, D. B. *J. Am. Chem. Soc.* **1996**, *118*, 10707−10718.
(8) Rennels, R. A.; Maliakal, A. J.; Collum, D. B. *J. Am. Chem. Soc.* **1998**, *120*, 421−422.
(9) Remenar, J. F.; Lucht, B. L.; Collum, D. B. *J. Am. Chem. Soc.* **1997**, *119*, 5567−5572.
(10) Remenar, J. F.; Collum, D. B. *J. Am. Chem. Soc.* **1998**, *120*, 4081−4086.
(11) Lucht, B. L.; Collum, D. B. *J. Am. Chem. Soc.* **1996**, *118*, 2217−2225.
(12) (a) Juaristi, E.; Beck, A. K.; Hansen, J.; Matt, T.; Mukhopadhyay, T.; Simson, M.; Seebach, D. *Synthesis* **1993**, 1271−1290. (b) Seebach, D.; Sting, A. R.; Hoffman, M. *Angew. Chem., Int. Ed. Engl.* **1996**, *35*, 2708−2748. (c) Seebach, D. *Angew. Chem., Int. Ed. Engl.* **1988**, *27*, 1624−1654.
(13) Sato, D.; Kawasaki, H.; Shimada, I.; Arata, Y.; Okamura, K.; Date, T.; Koga, K. *J. Am. Chem. Soc.* **1992**, *114*, 761.
(14) Williard, P. G.; Sun, C. *J. Am. Chem. Soc.* **1997**, *119*, 11693−11694.
(15) (a) Hilmersson, G.; Davidsson, Ö. *J. Org. Chem.* **1995**, *60*, 7660−7669. (b) Arvidsson, P. I.; Davidsson, Ö. To be submitted for publication. (c) Hilmersson, G.; Ahlberg, P.; Davidsson, Ö. *J. Am. Chem. Soc.* **1996**, *118*, 3539.
(16) Mukaiyama, T.; Asami, M. Chiral Pyrrolidine Diamines as Effective Ligands in Asymmetric Synthesis. In *Topics in Current Chemistry*; Boschke, D. F. L., Ed.; Springer-Verlag: Berlin, Heidelberg, 1985; Vol. 127, pp 133−167.
(17) Asami, M. *Chem. Lett.* **1984**, 829−832.
(18) Asami, M.; Ishizaki, T.; Inoue, S. *Tetrahedron: Asymmetry* **1994**, *5*, 793−796.
(19) Asami, M.; Suga, T.; Honda, K.; Inoue, S. *Tetrahedron Lett.* **1997**, *38*, 6425−6428.
(20) Khan, A. Z. Q.; W. de Groot, R.; Arvidsson, P. I.; Davidsson, Ö. *Tetrahedron: Asymmetry* **1998**, *9*, 1223−1229.

10.1021/ja9827550 CCC: $18.00
Published on Web 02/20/1999

Scheme 1

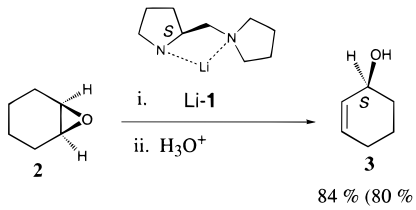

in THF has been reported to give the chiral alcohol (*S*)-**3** in both high yield and enantiomeric excess (Scheme 1). Solvents such as diethyl ether (DEE) or 2,5-dimethyltetrahydrofuran that are more sterically demanding than THF have been found to induce stereospecific proton-transfer reactions, in which cyclic allylic alcohols are transformed into homo allylic alcohols.[21−23]

Further mechanistic understanding and insights into the structures of these reagents are prerequisites for improved strategies in stereoselective synthesis with chiral lithium amides. In this paper we wish to report on novel structures and dynamics of coordination complexes of Li-**1** with diamine **1** and TMEDA.

Results and Discussion

Structure of the Chelate (Li-1)$_2$/1. The chiral lithium amide Li-**1** is prepared by addition of 1.0 equiv of *n*-Bu[^{6}Li] to a THF solution of (*S*)-2-(1-pyrrolidinylmethyl)pyrrolidine **1**. The NMR spectrum of Li-**1** in THF at low temperature shows a number of species undergoing exchange. In contrast, mixing **1** and *n*-BuLi in diethyl ether (DEE) immediately results in precipitation of Li-**1**. Presumably, Li-**1** forms aggregates with low solubility in DEE. However, addition of another 0.5 equiv of **1** to the mixture results in dissolution of the solid material, and the spectra shows sharp NMR resonances (^{1}H, ^{13}C, and ^{6}Li) at −90 °C. Nine carbon resonances are observed in DEE for Li-**1** and **1**, respectively. This shows that the rotation of the pyrrolidine rings of Li-**1** and **1** are slow on the NMR time scale (−90 °C). Thus, Li-**1** forms a complex with **1**. The intensities of the signals in the ^{13}C NMR spectrum show that Li-**1** and **1** forms a 2:1 chelate, i.e., (Li-**1**)$_2$/**1**.

In the ^{6}Li NMR spectrum of (Li-**1**)$_2$/**1** two resonances of equal intensity and line shape ($\nu_{1/2} \approx 1$ Hz) are observed at δ 1.83 and 2.65, respectively (Figure 1). The line shapes of the signals suggest that both lithiums are tetracoordinated.[15]

The overall results suggest that Li-**1** is a dimer, with one of its lithiums coordinated by the two pyrrolidine nitrogens in the amide ligands. The other lithium is chelated by the nitrogens in **1** (Figure 2).

The widely used lithium chelating diamine TMEDA is found to dissolve Li-**1** in DEE, presumably by formation of the complex shown in Figure 2. The ^{6}Li NMR spectrum of (Li-**1**)$_2$/**1** ([(Li-**1**)$_2$/**1**] = 0.1 M) displays lithium resonances at δ 1.34 and δ 2.46. However, TMEDA needs to be in excess (0.4 M) relative to Li-**1** to fully dissolve the crystals of Li-**1**, yielding (Li-**1**)$_2$/TMEDA. No monomers were observed.

There were no significant changes in the NMR spectrum upon addition of THF to the DEE solution of (Li-**1**)$_2$/**1**. This is clearly an indication that THF solvated (Li-**1**)$_2$ is not favored over (Li-**1**)$_2$/**1**. In a 2:1 mixture of THF:DEE the lithium signal at δ 1.83 was slightly broader than the signal at δ 2.65, indicating dynamic process involving coordination of THF.

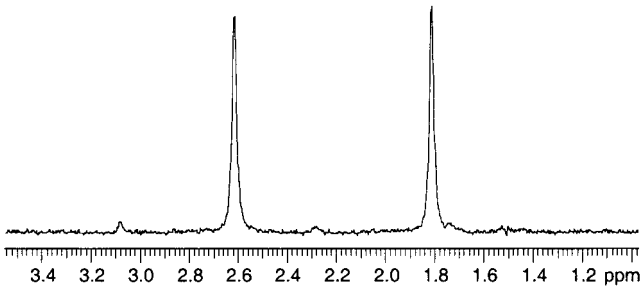

Figure 1. ^{6}Li NMR spectrum of (Li-**1**)$_2$/**1** at −91.5 °C in DEE-d_{10}.

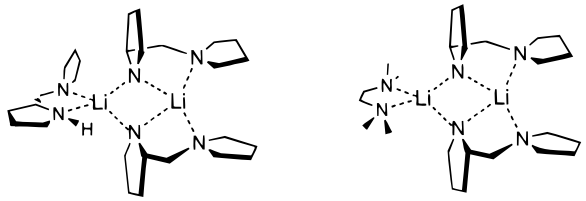

Figure 2. The dimer (Li-**1**)$_2$ solvated by **1** and TMEDA.

Li-**1** is soluble in THF, but the resulting NMR spectrum has broad, unresolved signals. However, addition of 1 equiv of **1** to a THF solution of Li-**1** gives rise to only two sharp ^{6}Li NMR resonances at δ 2.66 and 1.61. These resonances are of similar shape and shift to those of (Li-**1**)$_2$/**1** in the DEE:THF mixture above. In the ^{13}C spectrum at −105 °C both uncoordinated and coordinated **1** are observed. It is concluded that **1** is competitive with the bulk solvent THF for (Li-**1**)$_2$.

$$(\text{Li-}\mathbf{1})_2/\text{THF} + \mathbf{1} \overset{K}{\rightleftharpoons} (\text{Li-}\mathbf{1})_2/\mathbf{1} + \text{THF} \qquad \text{(I)}$$

From ^{13}C NMR intensities the equilibrium constant, *K* in eq I, is estimated to be 1×10^2. The disolvated (Li-**1**)$_2$/2THF is not considered due to the steric repulsions of two THF ligands coordinating (Li-**1**)$_2$ (cf. next section).

Computational Studies. A computational approach was employed to gain further insight into the structures and stabilities of the proposed structures for coordinated (Li-**1**)$_2$. The semi-empirical PM3 method[24] with Anders' lithium parameters[25] has been widely used in organolithium chemistry.[26,27] PM3 calculations have been shown to adequately reproduce geometries of organolithium compounds from experiments and higher level ab initio and density functional theory (DFT) methods.[28] However, the PM3 energies obtained are usually not as good.[29] Recently, Abbotto et al. showed that energies obtained by using density functional theory with the B3LYP hybrid functional with standard basis sets (6-31+G(d), 6-311+G(d)) on the PM3 optimized geometries (B3LYP/6-31G(d)//PM3) reproduce high level results (B3LYP/6-31G+(d)//B3LYP/6-31G+(d)) with high accuracy.[30] B3LYP//PM3 has now been applied beyond the size of small model systems to the study of large complexes such as (Li-**1**)$_2$/**1**.

(21) Khan, A. Z. Q.; Arvidsson, P. I.; Ahlberg, P. *Tetrahedron: Asymmetry* **1996**, *7*, 399−402.
(22) Nilsson Lill, S. O.; Arvidsson, P. I.; Ahlberg, P. *Acta Chem. Scand.* **1998**, *52*, 280−284.
(23) Arvidsson, P. I.; Hansson, M.; Khan, A. Z. Q.; Ahlberg, P. *Can. J. Chem.* **1998**, *76*, 795−799.
(24) Stewart, J. J. P. *J. Comput. Chem.* **1989**, *10*, 209.
(25) Anders, E.; Koch, R.; Freunscht, P. *J. Comput. Chem.* **1993**, *14*, 1301−1312.
(26) Opitz, A.; Koch, R.; Katritzky, A. R.; Fan, W.-Q.; Anders, E. *J. Org. Chem.* **1995**, *60*, 3743−3749.
(27) Koch, R.; Wiedel, B.; Anders, E. *J. Org. Chem.* **1996**, *61*, 2523−2529.
(28) Hilmersson, G.; Arvidsson, P. I.; Davidsson, Ö.; Håkansson, M. *J. Am. Chem. Soc.* **1998**, *120*, 8143−8149.
(29) Weiss, H.; Yakimansky, A. V.; Müller, A. H. E. *J. Am. Chem. Soc.* **1996**, *118*, 8897−8903.
(30) Abbotto, A.; Streitwieser, A.; Schleyer, P. v. R. *J. Am. Chem. Soc.* **1997**, *119*, 11255−11268.

Table 1. PM3 and B3LYP/6-31+G(d) Complexation Energies[a] for the Dimer (Li-**1**)$_2$ with Different Ligands **L**

$$(\text{Li-}\mathbf{1})_2 + \mathbf{L} \rightleftharpoons (\text{Li-}\mathbf{1})_2/\mathbf{L}$$

L	PM3	B3LYP/ 6-31+G(d)//PM3
Me_2O	−9.891	−8.253
TMEDA	−15.55	−13.94
1	−19.60	−18.15

[a] Energies in kcal mol^{-1}.

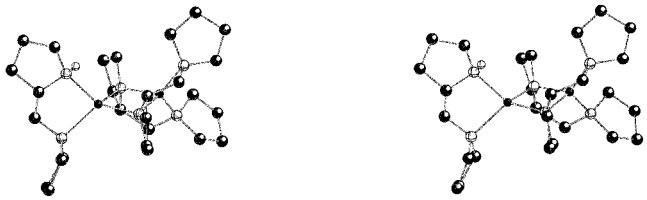

Figure 3. Ball and stick stereoview of the (Li-**1**)$_2$/**1** complex (PM3 optimized geometry).

The B3LYP/6-31+G(d)//PM3 complexation energies for complexes between (Li-**1**)$_2$ and dimethyl ether (used instead of DEE), TMEDA, and **1** are given in Table 1.

The B3LYP/6-31+G(d)//PM3 complexation energies are somewhat lower than those from PM3. Complexation of the dimer (Li-**1**)$_2$ with one molecule of dimethyl ether results in a net stabilization by 8.25 kcal mol^{-1}. Addition of a second ether molecule to get a dimer with both lithiums tetracoordinated resulted in a net destabilization by 1.65 kcal mol^{-1} on the PM3 level. Therefore, such a complex has not been considered further.

Complexation by one TMEDA molecule results in 13.9 kcal mol^{-1} of stabilization. Thus, TMEDA-solvated (Li-**1**)$_2$ is favored by 5.7 kcal mol^{-1} compared to that of the dimethyl ether complex. In agreement with the NMR results, the coordination of amine **1** to (Li-**1**)$_2$ yields the most stable complex. The complexation of **1** to form (Li-**1**)$_2$/**1** is favored by 4.2 kcal mol^{-1} compared to the (Li-**1**)$_2$/TMEDA complex.

One could imagine that addition of an additional equivalent of **1** would disrupt the dimer and yield diamine-coordinated monomeric amides, i.e., Li-**1**/**1** as previously reported for lithium amides without internal coordinating groups.[7] However, such a process is found to be endothermic by 3.8 kcal mol^{-1} (B3LYP level).

The PM3-optimized structure of (Li-**1**)$_2$/**1** is shown in Figure 3. (A stereoisomer of this complex in which the secondary nitrogen inverted is also possible, but this complex is higher in energy by 1.6 kcal mol^{-1}.) The two amides form a "C_2-symmetric" dimer, with a nearly planar (Li−N)$_2$ arrangement. This plane is almost perpendicular to the plane defined by one lithium atom and the two nitrogen atoms in the solvating diamine. The bond lengths and angles are typical, Figure 4.

Dynamic Studies of Ligand Exchange in (Li-1)$_2$/1. The ^{13}C NMR resonances for the complexed **1** in (Li-**1**)$_2$/**1** appear shifted relative to the signals for uncomplexed **1** in DEE at −105 °C. The signals for **1** in (Li-**1**)$_2$/**1** broaden upon addition of **1**, indicating slow ligand exchange on the NMR time scale. At −98 °C coalescence results, corresponding to a $\Delta G^{\ddagger}_{175K}$ of 7.8 kcal mol^{-1} for the ligand exchange. The rate constant for exchange is concentration independent in the interval 10 to 500 mM of uncomplexed diamine. This shows that the ligand exchange follows a dissociative mechanism. The chemical shifts and shapes of the other ^{13}C and ^{6}Li signals from Li-**1** are unaffected by further addition of **1**.

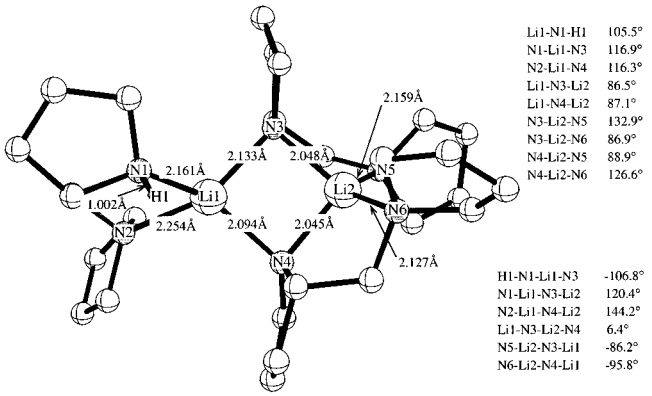

Figure 4. Structural features of the PM3 optimized geometry of (Li-**1**)$_2$/**1**. Hydrogens are omitted for clarity.

Dynamic Studies of Diamine−Amide Interconversion in (Li-1)$_2$/1. At ambient temperatures only one set of ^{13}C NMR resonances for **1** and Li-**1** is observed, indicating rapid interconversion of diamine and amide. The interconversion is due to the degenerate lithiation by Li-**1** of the diamine **1**. The coalescence temperature for the signals of the carbons in Li-**1** and coordinated **1** is approximately 268 K corresponding to a free energy of activation of 10.9 kcal mol^{-1}. (The rate constant for the diamine−amide interconversion at the coalescence temperature was obtained from complete line shape analysis of the ^{13}C NMR spectrum at 268 K. In the simulation the following populations were used: $\mathbf{1}_{\text{uncoord}} = 0.25$, $\mathbf{1}_{\text{coord}} = 0.25$, and Li-**1** = 0.5. Fast exchange between uncoordinated and coordinated **1** was assumed.)

We have shown two mechanisms for the degenerate diamine−amide interconversion. An intracomplex reaction within the chelate (Li-**1**)$_2$/**1** is depicted in eq II

$$(\text{Li-}\mathbf{1})_2/\mathbf{1}^* \overset{\text{exchange}}{\rightleftharpoons} (\text{Li-}\mathbf{1})(\text{Li-}\mathbf{1}^*)/\mathbf{1} \qquad \text{(II)}$$

A dissociative mechanism proceeding via two monomers solvated by **1** is shown in eq III. Such monomers may then undergo fast diamine−amide interconversion.

$$\begin{array}{ccc} (\text{Li-}\mathbf{1})_2/\mathbf{1}^* + \mathbf{1} & & (\text{Li-}\mathbf{1})(\text{Li-}\mathbf{1}^*)/\mathbf{1} + \mathbf{1} \\ \uparrow\downarrow & & \uparrow\downarrow \\ (\text{Li-}\mathbf{1})/\mathbf{1}^* + (\text{Li-}\mathbf{1})/\mathbf{1} & \overset{\text{exchange}}{\rightleftharpoons} & (\text{Li-}\mathbf{1}^*)/\mathbf{1} + (\text{Li-}\mathbf{1})/\mathbf{1} \end{array} \qquad \text{(III)}$$

These two mechanisms could be distinguished experimentally, since the rate for the process in eq III should show a concentration dependence on **1** while the process in eq II should not. The rate constant for the diamine−amide interconversion was found to be concentration independent in the interval 0.30 to 0.03 M, indicating that the interconversion proceeds via eq II rather than eq III.

A possible pathway for the degenerate rearrangement diamine−amide interconversion is depicted in Scheme 2. Initially one of the amide nitrogens abstracts the nitrogen bonded proton from the chelating diamine and both lithiums become attached to the thus formed amide nitrogen. The newly formed diamine only coordinates one of the lithiums (Li*). The internally coordinated pyrrolidine of the second is rearranged to coordinate the other lithium. A consequence of this diamine−amide interconversion via the depicted pathway in Scheme 2 is that the two lithiums have exchanged.

Dynamic Studies of Li−Li Exchange in (Li-1)$_2$/1. ^{6}Li,^{6}Li-EXSY experiments were performed on solutions of (Li-**1**)$_2$/**1** at −91 °C. The intensities of the cross-peak vs the diagonal

Scheme 2

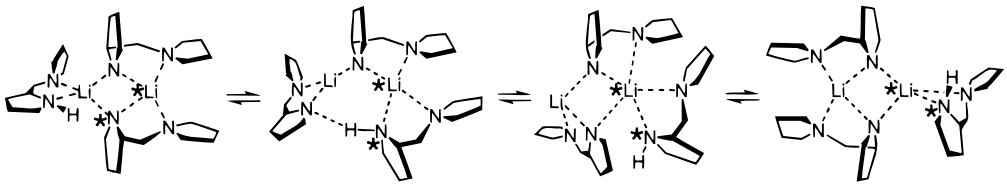

peak in the EXSY spectra with short mixing times ($\tau_m = 0.06-0.7$ s) were used to estimate the rate constant for the lithium exchange at −91 °C $k_{exch,182K} = 0.5$ s^{-1} and at −66 °C $k_{exch,207K} = 22$ s^{-1}, respectively.[31] This corresponds to $\Delta G^{\ddagger}_{182K}$ of 10.7 kcal mol^{-1} and $\Delta G^{\ddagger}_{207K} = 10.7$ kcal mol^{-1}. The two signals coalesce at −48 °C, corresponding to a $\Delta G^{\ddagger}_{225K}$ of 10.6 kcal mol^{-1}. These results show that the entropy of activation is close to zero for this process. Furthermore, the rate constants for the lithium exchange are practically independent of the concentration of uncoordinated diamine. Increasing the uncoordinated amine concentration $[\mathbf{1}]_{free}$ from approximately 10 mM to 500 mM resulted in less than a 2-fold increase of the rate constant. Therefore, the major pathway for the lithium exchange does not involve free amine. The exchange rate constant is also independent of [(Li-**1**)$_2$/**1**] in the interval 0.30 to 0.03 M. These results are consistent with an intramolecular lithium exchange mechanism. The similarity of the barrier for Li−Li exchange ($\Delta G^{\ddagger}_{182K} = 10.7$ kcal mol^{-1}) and the diamine−amide interconversion ($\Delta G^{\ddagger}_{268K} = 10.9$ kcal mol^{-1}) suggests that these processes are coupled, as shown in Scheme 2. The coordinated diamine catalyzes the intramolecular lithium−lithium exchange.

Since the above amine−amide interconversion mechanism is not available for the TMEDA complex, the mechanism for the lithium exchange must be different. The activation energy for the lithium exchange in the (Li-**1**)$_2$/TMEDA chelate was determined from the coalescence and found to be lower ($\Delta G^{\ddagger}_{213K} = 9.8$ kcal mol^{-1}) than that for the (Li-**1**)$_2$/**1** chelate ($\Delta G^{\ddagger}_{182K} = 10.7$ kcal mol^{-1}). However, it is important to keep in mind the large calculated difference in stability of the (Li-**1**)$_2$/**1** and (Li-**1**)$_2$/TMEDA chelates. The lithium exchange may proceed via uncomplexed (Li-**1**)$_2$, which rearranges its pyrrolidine ligands from one lithium to the other.[15a]

Furthermore, the coalescence temperature for the lithium exchange in (Li-**1**)$_2$/**1** in a 2:1 mixture of THF:DEE was observed at 207 K, only 10 degrees lower than that in pure DEE, indicating that the energy barrier for the lithium exchange is lowered by only 0.5 kcal mol^{-1}. Thus, THF only accelerates the lithium exchange by a factor of 3.5. This suggests that the major pathway for the lithium exchange in (Li-**1**)$_2$/**1** is the same in THF as in DEE solutions.

Conclusion

Novel types of structures composed of a diamine coordinating a dimeric complex of a chiral lithium amide have been presented. A number of dynamic processes have been studied by dynamic NMR spectroscopy. These include the following: lithium−lithium exchange, diamine ligand exchange, and degenerate diamine−amide interconversion, associated with a chelate of the type (Li-**1**)$_2$/**1**. The chiral diamine **1** catalyzes intramolecular lithium−lithium exchange when coordinated in the complex (Li-**1**)$_2$/**1**. Detailed mechanisms for the processes are presented.

The results described here provide insight into a new type of complex that may influence the reactivity of lithium amides. Mixtures containing both secondary amines and lithium amides often result when these reagents are used. Chiral bases often contain a chelating or coordinating group. Consequently, complexes of the kind reported here are likely to be present in the reaction mixture from, e.g., asymmetric enolization, deprotonation, and lithiation reactions. Our observation that the bidentate amine coordinates strongly to the dimer of the lithium amide raises the question if the chiral amine itself could act as a catalyst in lithiation reactions. Complexes of this type are likely to play crucial roles in the chemistry of organolithium amides.

Experimental Section

General. All syringes and NMR tubes used were dried overnight at 50 °C in a vacuum oven before transfer into a glovebox (Mecaplex GB 80 equipped with a gas purification system that removes oxygen and moisture) containing a nitrogen atmosphere. Typical moisture content was less than 0.5 ppm. All manipulations of the lithium compounds were carried out in the glovebox with gastight syringes. Deuterated ethereal solvents were stored and freshly distilled from Deporex (Fluka AG) prior to use. TMEDA (Aldrich) was distilled from calcium hydride in nitrogen atmosphere.

Preparation of (*S*)-2-(1-Pyrrolidinylmethyl)pyrrolidine. This compound was prepared according to literature methods.[32]

Preparation of [^{6}Li]-Butyllithium. This compound was prepared according to the literature.[33]

NMR. All NMR experiments were performed in Wilmad (5 mm) tubes fitted with a Wilmad/Omnifit Teflon valve assembly (OFV) with a Teflon/silicone septum. NMR spectra were recorded with a Varian Unity 500 spectrometer equipped with three channels with a 5-mm ^{1}H,^{13}C,^{6}Li triple resonance probe head custom built by Nalorac. Measuring frequencies were 500 (^{1}H) and 74 MHz (^{6}Li). The ^{1}H and ^{13}C spectra were referenced to the solvent signals: DEE-d_{10} δ 1.06 ($-CD_2{}^1H$) and δ 14.60 ($-{}^{13}CD_3$), respectively. Lithium spectra were referenced to external 0.3 M [^{6}Li]Cl in MeOH-d_4 ($\delta = 0.0$). A typical 90° ^{6}Li pulse was 20 μs. Probe temperatures were measured after more than 1 h of temperature equilibration with both a calibrated methanol-Freon NMR thermometer[34] and the standard methanol thermometer supplied by Varian instruments.

Computational Methods. PM3[24] geometry optimizations, with parameters for lithium,[25] were done on a Silicon Graphics Power Indigo 2 workstation with the Spartan 5.0 program package.[35] Several initial geometries for the optimizations were tried to find the global minimum. The structures were then reoptimized by using the keyword HHon, to eliminate the overly positive HH attraction of the PM3 method.[36,37] The vibrational frequencies were also calculated to verify that all optimized structures were minima on the potential energy surface. Single point energies, calculated by using density functional theory (DFT)

(31) Perrin, C. L.; Dwyer, T. J. *Chem. Rev.* **1990**, *90*, 935−967.
(32) Asami, M. *Bull. Chem. Soc. Jpn.* **1990**, *63*, 721−727.
(33) Hilmersson, G.; Davidsson, Ö. *J. Organomet. Chem.* **1995**, *489*, 175−179.
(34) Engdahl, C.; Ahlberg, P. *J. Am. Chem. Soc.* **1979**, *101*, 3940.
(35) *SPARTAN*; Version 5.0.1; Wavefunction, Inc.: 18401 Von Karman Ave., #370 Irvine, CA 92715, 1995.
(36) Huang, W. Personal communication.
(37) Csonka, G. I. *J. Comput. Chem.* **1993**, *14*, 895−898.

employing the B3LYP hybrid functional[38] with the SCF=tight keyword on the PM3 optimized structures, were done on a Cray C90 computer using the Gaussian 94 program package.[39] The standard valence double-ζ basis set 6-31+G(d)[40] was used as implemented in the program.

(38) Becke, A. D. *J. Chem. Phys.* **1993**, *98*, 5648.

(39) *Gaussian 94*; Revision C.3; Frisch, M. J.; Trucks, G. W.; Schlegel, H. B.; Gill, P. M. W.; Johnson, B. G.; Robb, M. A.; Cheeseman, J. R.; Keith, T.; Petersson, G. A.; Montgomery, J. A.; Raghavachari, K.; Al-Laham, M. A.; Zakrzewski, V. G.; Ortiz, J. V.; Foresman, J. B.; Cioslowski, J.; Stefanov, B. B.; Nanayakkara, A.; Challacombe, M.; Peng, C. Y.; Ayala, P. Y.; Chen, W.; Wong, M. W.; Andres, J. L.; Replogle, E. S.; Gomperts, R.; Martin, R. L.; Fox, D. J.; Binkley, J. S.; Defrees, D. J.; Baker, J.; Stewart, J. P.; Head-Gordon, M.; Gonzalez, C.; Pople, J. A.; Gaussian, Inc.: Pittsburgh, PA, 1995.

(40) Spitznagel, G. W.; Clark, T.; Chandrasekhar, J.; Schleyer, P. v. R. *J. Comput. Chem.* **1982**, *3*, 363.

Acknowledgment. We are grateful to the Swedish Natural Science Research Council for financial support and to Nationell Superdatorcentrum (NSC), Linköping, Sweden for computer time. We thank Öjvind Davidsson for helpful discussions. Linguistic improvements suggested by the reviewers are also acknowledged.

Supporting Information Available: Tables of Cartesian coordinates and energies for the calculated structures (PDF). This material is available free of charge via the Internet at http://pubs.acs.org.

JA9827550